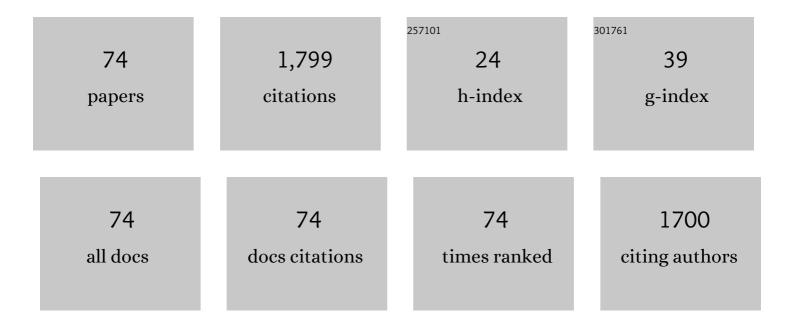
## Jijie Huang

List of Publications by Year in descending order

Source: https://exaly.com/author-pdf/2805983/publications.pdf Version: 2024-02-01



LULE HUANC

#	Article	IF	CITATIONS
1	Two-dimensional nanofluidics. Science, 2016, 351, 1395-1396.	6.0	260
2	Self-Assembled Epitaxial Au–Oxide Vertically Aligned Nanocomposites for Nanoscale Metamaterials. Nano Letters, 2016, 16, 3936-3943.	4.5	91
3	New epitaxy paradigm in epitaxial self-assembled oxide vertically aligned nanocomposite thin films. Journal of Materials Research, 2017, 32, 4054-4066.	1.2	86
4	Self-assembled Co–BaZrO <sub>3</sub> nanocomposite thin films with ultra-fine vertically aligned Co nanopillars. Nanoscale, 2017, 9, 7970-7976.	2.8	64
5	Multifunctional La <sub>0.67</sub> Sr <sub>0.33</sub> MnO <sub>3</sub> (LSMO) Thin Films Integrated on Mica Substrates toward Flexible Spintronics and Electronics. ACS Applied Materials & Interfaces, 2018, 10, 42698-42705.	4.0	62
6	Three-dimensional strain engineering in epitaxial vertically aligned nanocomposite thin films with tunable magnetotransport properties. Materials Horizons, 2018, 5, 536-544.	6.4	57
7	Nanoscale Artificial Plasmonic Lattice in Selfâ€Assembled Vertically Aligned Nitride–Metal Hybrid Metamaterials. Advanced Science, 2018, 5, 1800416.	5.6	56
8	A high-performance bionic pressure memory device based on piezo-OLED and piezo-memristor as luminescence-fish neuromorphic tactile system. Nano Energy, 2020, 77, 105120.	8.2	41
9	High-Performance and Reliable Silver Nanotube Networks for Efficient and Large-Scale Transparent Electromagnetic Interference Shielding. ACS Applied Materials & Interfaces, 2021, 13, 15525-15535.	4.0	41
10	Single-Layer MoS <sub>2</sub> Mechanical Resonant Piezo-Sensors with High Mass Sensitivity. ACS Applied Materials & Interfaces, 2020, 12, 41991-41998.	4.0	39
11	Hybrid plasmonic Au–TiN vertically aligned nanocomposites: a nanoscale platform towards tunable optical sensing. Nanoscale Advances, 2019, 1, 1045-1054.	2.2	37
12	Selfâ€Organized Epitaxial Vertically Aligned Nanocomposites with Longâ€Range Ordering Enabled by Substrate Nanotemplating. Advanced Materials, 2017, 29, 1606861.	11.1	36
13	Exchange Bias in a La <sub>0.67</sub> Sr <sub>0.33</sub> MnO <sub>3</sub> /NiO Heterointerface Integrated on a Flexible Mica Substrate. ACS Applied Materials & Interfaces, 2020, 12, 39920-39925.	4.0	36
14	Self-assembled vertically aligned Ni nanopillars in CeO <sub>2</sub> with anisotropic magnetic and transport properties for energy applications. Nanoscale, 2018, 10, 17182-17188.	2.8	34
15	Exchange Bias Effect along Vertical Interfaces in La0.7Sr0.3MnO3:NiO Vertically Aligned Nanocomposite Thin Films Integrated on Silicon Substrates. Crystal Growth and Design, 2018, 18, 4388-4394.	1.4	33
16	Tailorable Optical Response of Au–LiNbO <sub>3</sub> Hybrid Metamaterial Thin Films for Optical Waveguide Applications. Advanced Optical Materials, 2018, 6, 1800510.	3.6	32
17	Selfâ€Assembled Ag–TiN Hybrid Plasmonic Metamaterial: Tailorable Tilted Nanopillar and Optical Properties. Advanced Optical Materials, 2019, 7, 1801180.	3.6	31
18	Plasmonic Cu nanostructures in ZnO as hyperbolic metamaterial thin films. Materials Today Nano, 2019, 8, 100052.	2.3	30

JIJIE HUANG

#	Article	IF	CITATIONS
19	Strain-driven nanodumbbell structure and enhanced physical properties in hybrid vertically aligned nanocomposite thin films. Applied Materials Today, 2019, 16, 204-212.	2.3	30
20	Vertically Aligned Nanocomposite BaTiO <sub>3</sub> :YMnO <sub>3</sub> Thin Films with Room Temperature Multiferroic Properties toward Nanoscale Memory Devices. ACS Applied Nano Materials, 2018, 1, 2509-2514.	2.4	29
21	Microscopic adaptation of BaHfO <sub>3</sub> and Y <sub>2</sub> O <sub>3</sub> artificial pinning centers for strong and isotropic pinning landscape in YBa <sub>2</sub> Cu <sub>3</sub> O <sub>7–<i>x</i></sub> thin films. Superconductor Science and Technology. 2018. 31. 025008.	1.8	27
22	Broad Range Tuning of Phase Transition Property in VO <sub>2</sub> Through Metal eramic Nanocomposite Design. Advanced Functional Materials, 2019, 29, 1903690.	7.8	26
23	Multifunctional Metal–Oxide Nanocomposite Thin Film with Plasmonic Au Nanopillars Embedded in Magnetic La <sub>0.67</sub> Sr <sub>0.33</sub> MnO <sub>3</sub> Matrix. Nano Letters, 2021, 21, 1032-1039.	4.5	26
24	Magnetic properties of (CoFe2O4)x:(CeO2)1â^'x vertically aligned nanocomposites and their pinning properties in YBa2Cu3O7â^´Î´thin films. Journal of Applied Physics, 2014, 115, 123902.	1.1	25
25	A simplified superconducting coated conductor design with Fe-based superconductors on glass and flexible metallic substrates. Journal of Alloys and Compounds, 2015, 647, 380-385.	2.8	25
26	Novel Layered Supercell Structure from Bi <sub>2</sub> AlMnO <sub>6</sub> for Multifunctionalities. Nano Letters, 2017, 17, 6575-6582.	4.5	25
27	Microstructure, Magnetic, and Magnetoresistance Properties of La0.7Sr0.3MnO3:CuO Nanocomposite Thin Films. ACS Applied Materials & Interfaces, 2018, 10, 5779-5784.	4.0	24
28	Tailoring physical functionalities of complex oxides by vertically aligned nanocomposite thin-film design. MRS Bulletin, 2021, 46, 159-167.	1.7	23
29	Strong perpendicular exchange bias in epitaxial La0.7Sr0.3MnO3:LaFeO3 nanocomposite thin films. APL Materials, 2016, 4, .	2.2	22
30	Probing the effect of interface on vortex pinning efficiency of one-dimensional BaZrO3 and BaHfO3 artificial pinning centers in YBa2Cu3O7-x thin films. Applied Physics Letters, 2018, 113, .	1.5	22
31	60Ânm Pixel-size pressure piezo-memory system as ultrahigh-resolution neuromorphic tactile sensor for in-chip computing. Nano Energy, 2021, 87, 106190.	8.2	21
32	Transformational dynamics of BZO and BHO nanorods imposed by Y2O3 nanoparticles for improved isotropic pinning in YBa2Cu3O7-δ thin films. AIP Advances, 2017, 7, .	0.6	20
33	Effective magnetic pinning schemes for enhanced superconducting property in high temperature superconductor YBa <sub>2</sub> Cu <sub>3</sub> O <sub>7â^'<i>x</i></sub> : a review. Superconductor Science and Technology, 2017, 30, 114004.	1.8	19
34	3D Hybrid Plasmonic Framework with Au Nanopillars Embedded in Nitride Multilayers Integrated on Si. Advanced Materials Interfaces, 2020, 7, 2000493.	1.9	18
35	Multifunctional self-assembled BaTiO3-Au nanocomposite thin films on flexible mica substrates with tunable optical properties. Applied Materials Today, 2020, 21, 100856.	2.3	17
36	Monolayer MXene Nanoelectromechanical Piezoâ€Resonators with 0.2 Zeptogram Mass Resolution. Advanced Science, 2022, 9, .	5.6	17

JIJIE HUANG

#	Article	IF	CITATIONS
37	Enhanced superconducting properties of YBa2Cu3O7â^î´thin film with magnetic nanolayer additions. Ceramics International, 2016, 42, 12202-12209.	2.3	16
38	Tunable magnetic anisotropy of self-assembled Fe nanostructures within a La0.5Sr0.5FeO3 matrix. Applied Physics Letters, 2018, 112, .	1.5	16
39	Strain and property tuning of the 3D framed epitaxial nanocomposite thin films via interlayer thickness variation. Journal of Applied Physics, 2019, 125, .	1.1	16
40	Tunable low-field magnetoresistance properties in (La0.7Ca0.3MnO3)1â^'x:(CeO2)x vertically aligned nanocomposite thin films. Applied Physics Letters, 2019, 115, 053103.	1.5	15
41	Tuning magnetic anisotropy in Co–BaZrO <sub>3</sub> vertically aligned nanocomposites for memory device integration. Nanoscale Advances, 2019, 1, 4450-4458.	2.2	15
42	Thermally Stable Au–BaTiO <sub>3</sub> Nanoscale Hybrid Metamaterial for High-Temperature Plasmonic Applications. ACS Applied Nano Materials, 2020, 3, 1431-1437.	2.4	15
43	Upper Critical Field and Kondo Effects in Fe(Te0.9Se0.1) Thin Films by Pulsed Field Measurements. Scientific Reports, 2016, 6, 21469.	1.6	14
44	Multiferroic vertically aligned nanocomposite with CoFe2O4 nanocones embedded in layered Bi2WO6 matrix. Materials Research Letters, 2019, 7, 418-425.	4.1	14
45	Highâ€Ðynamicâ€Range Pressure Mapping Interactions by Dual Piezoâ€Phototronic Transistor with Piezoâ€Nanowire Channels and Piezoâ€OLED Gates. Advanced Functional Materials, 2020, 30, 2004724.	7.8	14
46	Core-shell metallic alloy nanopillars-in-dielectric hybrid metamaterials with magneto-plasmonic coupling. Materials Today, 2021, 51, 39-47.	8.3	14
47	Room temperature magnetodielectric effects in epitaxial hexaferrite BaFe10.2Sc1.8O19 thin film. Applied Physics Letters, 2017, 110, .	1.5	11
48	Li <sub>2</sub> MnO <sub>3</sub> Thin Films with Tilted Domain Structure as Cathode for Li-Ion Batteries. ACS Applied Energy Materials, 2019, 2, 3461-3468.	2.5	11
49	Freestanding La <sub>0.7</sub> Sr <sub>0.3</sub> MnO <sub>3</sub> :NiO vertically aligned nanocomposite thin films for flexible perpendicular interfacial exchange coupling. Materials Research Letters, 2022, 10, 287-294.	4.1	11
50	Epitaxial TiN/MgO multilayers with ultrathin TiN and MgO layers as hyperbolic metamaterials in visible region. Materials Today Physics, 2021, 16, 100316.	2.9	10
51	Strategies To Construct <i>n</i> -Type Si-Based Heterojunctions for Photoelectrochemical Water Oxidation. , 2022, 4, 779-804.		10
52	Magnetic (CoFe2O4)0.1(CeO2)0.9nanocomposite as effective pinning centers in FeSe0.1Te0.9thin films. Journal of Physics Condensed Matter, 2016, 28, 025702.	0.7	9
53	Two-Phase Room-Temperature Multiferroic Nanocomposite with BiMnO3-Tilted Nanopillars in the Bi2W1–xMnxO6 Matrix. ACS Applied Materials & Interfaces, 2019, 11, 26261-26267.	4.0	9
54	Novel vertically aligned nanocomposite of Bi2WO6-Co3O4 with room-temperature multiferroic and anisotropic optical response. Nano Research, 0, , 1.	5.8	9

Jijie Huang

#	Article	IF	CITATIONS
55	Superconducting Iron Chalcogenide Thin Films Integrated on Flexible Mica Substrates. IEEE Transactions on Applied Superconductivity, 2019, 29, 1-4.	1.1	8
56	Tailorable Fe nanostructures and magnetic anisotropy in (La0.5Sr0.5FeO3)1-x:Fex thin films integrated on SrTiO3 and silicon substrates. Materials Today Advances, 2020, 8, 100112.	2.5	8
57	Multiferroic thin film via SrRuO3–BaTiO3 vertically aligned nanocomposite design. Applied Physics Letters, 2020, 117, .	1.5	8
58	Enhanced Flux Pinning Properties of YBCO Thin Films With Various Pinning Landscapes. IEEE Transactions on Applied Superconductivity, 2017, 27, 1-5.	1,1	7
59	Comparison Study of the Flux Pinning Enhancement of YBa <sub>2</sub> Cu <sub>3</sub> O <sub>7â~î</sub> Thin Films With BaHfO <sub>3</sub> + Y <sub>2</sub> O <sub>3</sub> Single- and Mixed-Phase Additions. IEEE Transactions on Applied Superconductivity. 2019. 29. 1-5.	1.1	7
60	Role of Interlayer in 3D Vertically Aligned Nanocomposite Frameworks with Tunable Magnetotransport Properties. Advanced Materials Interfaces, 2020, 7, 1901990.	1.9	7
61	Interfacial Engineering Enabled Novel Bi-Based Layered Oxide Supercells with Modulated Microstructures and Tunable Physical Properties. Crystal Growth and Design, 2019, 19, 7088-7095.	1.4	6
62	Room-Temperature Ferroelectric LiNb <sub>6</sub> Ba <sub>5</sub> Ti <sub>4</sub> O <sub>30</sub> Spinel Phase in a Nanocomposite Thin Film Form for Nonlinear Photonics. ACS Applied Materials & Interfaces, 2020, 12, 23076-23083.	4.0	6
63	Double-Exchange Bias Modulation under Horizontal and Perpendicular Field Directions by 3D Nanocomposite Design. ACS Applied Materials & Interfaces, 2021, 13, 50141-50148.	4.0	6
64	High-performance fully-stretchable solid-state lithium-ion battery with a nanowire-network configuration and crosslinked hydrogel. Journal of Materials Chemistry A, 2022, 10, 11562-11573.	5.2	6
65	Effective doping control in Sm-doped BiFeO <sub>3</sub> thin films <i>via</i> deposition temperature. RSC Advances, 2020, 10, 40229-40233.	1.7	5
66	Metal-Nitride nanocomposite thin film of nanomaze-like Cu embedded in TiN. Materials Letters, 2021, 294, 129780.	1.3	4
67	Integration of Self-Assembled BaZrO <sub>3</sub> -Co Vertically Aligned Nanocomposites on Mica Substrates toward Flexible Spintronics. Crystal Growth and Design, 2022, 22, 718-725.	1.4	4
68	Enhanced Flux Pinning Properties in \$hbox{YBa}_{2}hbox{Cu}_{3}hbox{O}_{7-delta}\$/ \$(hbox{CoFe}_{2}hbox{O}_{4})_{0.3}(hbox{CeO}_{2})_{0.7} \$ Multilayer Thin Films. IEEE Transactions on Applied Superconductivity, 2015, 25, 1-4.	1.1	2
69	Multifunctional Cu–BaTiO3 nanocomposite thin film fabricated via pulsed laser deposition. Ceramics International, 2020, 46, 25817-25821.	2.3	1
70	Exchange Bias Effect in LaFeO3: La0.7Ca0.3MnO3 Composite Thin Films. Coatings, 2021, 11, 1125.	1.2	1
71	Flexible La0.67Sr0.33MnO3:ZnO Nanocomposite Thin Films Integrated on Mica. Frontiers in Materials, 2022, 9, .	1.2	1
72	Si integration of La <sub>0.7</sub> Sr <sub>0.3</sub> MnO <sub>3</sub> :BiFeO <sub>3</sub> nanocomposite thin films with strong exchange bias coupling. Applied Physics Letters, 2022, 121, 022403.	1.5	1

#	Article	IF	CITATIONS
73	Industrial pulsed laser deposition for ultra-fast growth of high-temperature superconducting thin films with nanostructured pinning centers. Superconductor Science and Technology, 2021, 34, 080501.	1.8	0
74	Interface superconductivity in PLD grown FeSe/SrTiO3 heterostructure. Superconductor Science and Technology, 0, , .	1.8	0